# SKIN-FRICTION DRAG REDUCTION DESCRIBED VIA THE ANISOTROPIC GENERALISED KOLMOGOROV EQUATIONS

**A. Chiarini & M. Quadrio**

Department of Aerospace Sciences and Technologies, Politecnico di Milano, via La Masa 34, 20156 Milano, Italy

**D. Gatti**

Institute of Fluid Mechanics, Karlsruhe Institute of Technology, 76131 Karlsruhe, Germany

In the present work, the recently introduced [1] Anisotropic Generalised Kolmogorov Equations, or AGKE, are used to investigate how skin-friction drag reduction alters the inter-component and multiscale processes of turbulence.

The AGKE are budget equations for the second-order structure function tensor $\langle \delta u_i \delta u_j \rangle$, where $\delta u_i$ is the increment of the $i$-th velocity component at position $\boldsymbol{X}$ and separation $\boldsymbol{r}$, i.e. $\delta u_i = u_i\left(\boldsymbol{X} + \boldsymbol{r}/2\right) - u_i\left(\boldsymbol{X} - \boldsymbol{r}/2\right)$. In the general case, $\langle \delta u_i \delta u_j \rangle$ depends upon time and six independent spatial variables, i.e. the six coordinates of $\boldsymbol{X}$ and $\boldsymbol{r}$; they reduce to four in the indefinite plane channel geometry. The AGKE read:

$$\frac{\partial \langle \delta u_i \delta u_j \rangle}{\partial t} + \frac{\partial \phi_{k,ij}}{\partial r_k} + \frac{\partial \psi_{k,ij}}{\partial X_k} = P_{ij} + \Pi_{ij} + D_{ij} \qquad (1)$$

where $\boldsymbol{\phi}_{ij}$ and $\boldsymbol{\psi}_{ij}$ are fluxes of $\langle \delta u_i \delta u_j \rangle$ along directions of statistical inhomogeneity and among scales respectively, and $P_{ij}$, $\Pi_{ij}$ and $D_{ij}$ denote the production, pressure strain and viscous dissipation. Overall, the AGKE describe the production, transport and dissipation of the components of the scale Reynolds stresses in the combined physical ($\boldsymbol{X}$) and scale ($\boldsymbol{r}$) space and in time ($t$), and bring to light properties of the turbulent flows which can not be highlighted by conventional single-point budgets or spectra.

Figure 1 is a typical AGKE result for a statistically stationary turbulent channel flow. As in such flow the only statistically non-homogeneous direction is the wall-normal one, the AGKE terms are defined in the $(r_x, r_y, r_z, Y)$ four-dimensional space; $x$, $y$ and $z$ denote the streamwise, wall-normal and spanwise directions. Additionally, the space of wall-normal scales is defined only for $|r_y|/2 < Y$, owing to the finite extension of the channel in the wall-normal direction. Figure 1 shows the source term of $\langle -\delta u \delta v \rangle$, i.e. the r.h.s. of Eq.1: $\xi_{12} = P_{12} + \Pi_{12} + D_{12}$, in the $r_x = 0$ space. Large positive and negative values of $\xi_{12}$ are found to define two distinct regions in the buffer layer, both involving small wall-normal scales $r_y$. The region with positive $\xi_{12}$ corresponds to intermediate spanwise scales ($10 \le r_z^+ \le 50$), and the other region to very small ones ($r_z^+ \sim 0$). In the buffer layer, except at the scales corresponding to the region of large positive values, $\xi_{12}$ is negative everywhere. On the contrary, at larger $Y$, $\xi_{12}$ is slightly positive at all scales. The positive and negative peaks of $\xi_{12}$, respectively placed at $(r_y^+, r_z^+, Y^+) \sim (0, 20, 13)$ and $(r_y^+, r_z^+, Y^+) \sim (19, 0, 12)$, highlight the different scales of maximum contribution; similarly to the budget of $\langle -uv \rangle$, as $D_{12}$ is negligible in the overall four-dimensional space, the
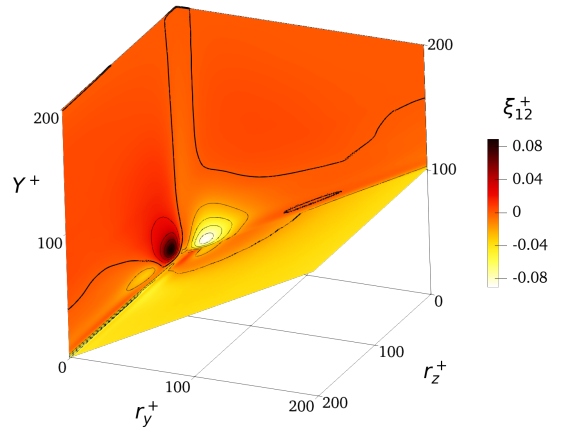


Figure 1: Colour plot of $\xi_{12}^+$ in the $r_x = 0$ space for a turbulent channel flow. Contour lines increment by 0.02, with zero indicated by a thick line.

positive contribution to $\xi_{12}$ entirely comes from $P_{12}$, whereas the negative one from $\Pi_{12}$.

Armed with this novel tool, we investigate how a well-known skin-friction drag reduction technique, namely the spanwise-oscillating wall [3], affects this picture. Two (with and without wall oscillations) Direct Numerical Simulations at Constant Power Input (CPI) [2] (carried out at a value of the power-based $Re$ equivalent to $Re_\tau = 200$ for the unforced flow) are carried out, with wall oscillation amplitude and period set at $A^+ = 4.5$ and $T^+ = 125.5$, i.e. near the maximum net energy saving condition [4]. Hereafter, unless otherwise indicated quantities are expressed in power units (see [2] for their definition), whereas the + superscript denotes quantities expressed in actual viscous units.

The comparison of AGKE terms in the controlled and non-controlled cases shows that the oscillating wall modifies production, transport and dissipation of the components of the $\langle \delta u_i \delta u_j \rangle$ tensor. For example, for the $\langle \delta u \delta u \rangle$ component, the oscillating wall shifts the main transfers towards larger wall-distances. This is shown in figure 2. Here the main field lines of fluxes $\phi_{11}$ and $\psi_{11}$, representative of the transfers of $\langle \delta u \delta u \rangle$ in space and among scales, are shown in the $r_x = r_z = 0$ plane for both the controlled and non-controlled cases. In both cases these field lines originate in the buffer layer at $r_y = 0$. In the first part of their path they follow
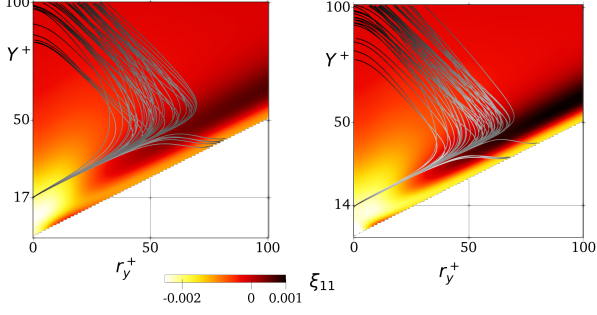
Figure 2: Colour plot of the source term $\xi_{11}$ of $\langle \delta u \delta u \rangle$ in the $r_x = r_z = 0$ space. Gray lines are tangent to the vector of the fluxes. Left: controlled case. Right: non-controlled case.
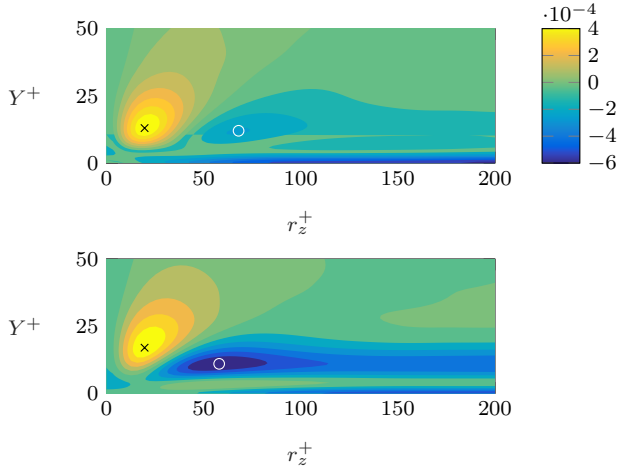


Figure 3: Colour plot of $\xi_{12}$ in the $r_x = r_y = 0$ plane. Top: Non-controlled case. Bottom: Controlled case. The black cross and white circle denote respectively the positions of the positive maximum and negative minimum of $\xi_{12}$ in the plane.

an oblique line described by $Y^+ = r_y^+/2 + K_{11}^+$, parallel to the lower boundary of the domain. This implies a transfer of $\langle \delta u \delta u \rangle$ towards larger wall-distances and towards larger wall-normal scales. Finally, they vanish at larger wall distances at null wall-normal scales, i.e. at the $r_y = 0$ axis, or in correspondence of the wall, i.e. in the lower boundary of the domain; accordingly, at the smallest scales and in the near-wall region $\langle \delta u \delta u \rangle$ is completely dissipated via viscous effects. The effect of the oscillating wall is clearly visible as a shift of these transfers towards larger wall-distances: $K_{11}^+$ is found to increase from 14 in the non-controlled case, to 17. Interestingly, such changes are not evident for the $\langle \delta v \delta v \rangle$ component: $K_{22}^+ = 40$ in both the controlled and non-controlled cases.

On the contrary, in the off-diagonal component $\langle -\delta u \delta v \rangle$ the oscillating wall changes the wall-normal location and spanwise scale of the maximum production $(P_{12,m})$ and those of the minimum pressure strain $(\Pi_{12,m})$, the main sink contributor. The latter is moved slightly closer to the wall, whereas the former away from; both occur at smaller $r_z$. This is shown in figure 3 where the source term $\xi_{12}$, for both the controlled and non-controlled cases, is shown in the $r_x = r_y = 0$ plane, and the positions of its maximum and minimum shown with symbols. The positive peak of $\xi_{12}$ shifts towards larger $Y$ and slightly smaller $r_z$ together with $P_{12,m}$, whereas its relative minimum in this plane shifts towards smaller $Y$ and smaller $r_z$, together with $\Pi_{12,m}$. The increased offset between the wall-
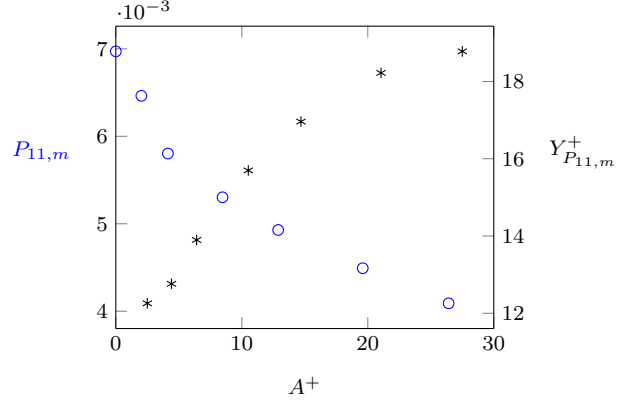


Figure 4: Dependence of the maximum of the production of $\langle \delta u \delta u \rangle$ $(P_{11,m})$ on the amplitude of the oscillating wall $(A)$. Blue circles: intensity (expressed in power units, left axis) versus $A^+$. Black asterisks: wall-normal position (expressed in actual wall units, right axis) versus $A^+$.

normal positions of $P_{12,m}$ and $\Pi_{12,m}$ results in a larger sink for $\langle -\delta u \delta v \rangle$ in the buffer layer at $r_z^+ > 40$ and $Y^+ \in (7, 20)$, and in a more intense source at slightly larger wall distances, in a region characterized by $r_z^+ > 150$ and $Y^+ \in (25, 50)$.

The most important changes in the AGKE statistics are then studied as a function on the amplitude of the oscillating wall (hence, indirectly, of the amount of drag reduction) in a second phase of the study. Six additional (smaller) DNSs are conducted where the amplitude of the oscillations is varied up to $A^+ = 30$. The analysis highlights several interesting trends. As an example, figure 4 shows how the maximum of the production of $\langle \delta u \delta u \rangle$ $(P_{11,m})$ and its position change with $A$. The value $P_{11,m}$ of the maximum is found to decrease with $A^+$. On the contrary, its wall-normal position $Y_{P_{11,m}}^+$ increases significantly with $A^+$ from $Y^+ \sim 12$ to $Y^+ \sim 19$, seemingly approaching an asymptotic value.

At the conference, the most important changes induced by flow control on the energy fluxes will be addressed, with a view to isolate the key mechanism behind skin-friction drag reduction.

**REFERENCES**

[1] D. Gatti, A. Chiarini, A. Cimarelli, and M. Quadrio. Production, transport and dissipation of turbulent stresses across scales and space. In *International Turbulence Initiative, Bertinoro (I), Sept. 5-7 2018*, 2018.

[2] Y. Hasegawa, M. Quadrio, and B. Frohnapfel. Numerical simulation of turbulent duct flows at constant power input. *J. Fluid Mech.*, 750:191–209, 2014.

[3] W.J. Jung, N. Mangiavacchi, and R. Akhavan. Suppression of turbulence in wall-bounded flows by high-frequency spanwise oscillations. *Phys. Fluids A*, 4 (8):1605–1607, 1992.

[4] M. Quadrio and P. Ricco. Critical assessment of turbulent drag reduction through spanwise wall oscillation. *J. Fluid Mech.*, 521:251–271, 2004.